DTU Library

Human In-vivo Brain MR Current Density Imaging (MRCDI) based on Steady-state Free Precession Free Induction Decay (SSFP-FID)

Göksu, Cihan; Hanson, Lars G. ; Siebner, Hartwig; Ehses, Philipp; Scheffler, Klaus; Thielscher, Axel

Publication date:
2018

Document Version
Publisher's PDF, also known as Version of record

Citation (APA):
Göksu, C., Hanson, L. G., Siebner, H., Ehses, P., Scheffler, K., & Thielscher, A. (2018). *Human In-vivo Brain MR Current Density Imaging (MRCDI) based on Steady-state Free Precession Free Induction Decay (SSFP-FID)*. Abstract from Joint Annual Meeting ISMRM-ESMRMB 2018, Paris, France.

0542

Human In-vivo Brain MR Current Density Imaging (MRCDI) based on Steady-state Free Precession Free Induction Decay (SSFP-FID)

Cihan Göksu[1,2], Lars G. Hanson[1,2], Hartwig R. Siebner[2,3], Philipp Ehses[4,5], Klaus Scheffler[4,6], and Axel Thielscher[1,2]

[1]Center for Magnetic Resonance, DTU Elektro, Technical University of Denmark, Kgs. Lyngby, Denmark, [2]Danish Research Centre for Magnetic Resonance, Centre for Functional and Diagnostic Imaging and Research, Copenhagen University Hospital, Hvidovre, Denmark, [3]Department of Neurology, Copenhagen University Hospital, Bispebjerg, Denmark, [4]High-Field Magnetic Resonance Center, Max-Planck-Institute for Biological Cybernetics, Tübingen, Germany, [5]German Center for Neurodegenerative Diseases (DZNE), Bonn, Germany, [6]Department of Biomedical Magnetic Resonance, University of Tübingen, Tübingen, Germany

Synopsis

MRCDI is a novel technique for non-invasive measurement of weak currents in the human head, which is important in several neuroscience applications. Here, we present reliable in-vivo MRCDI measurements in the human brain based on SSFP-FID, yielding an unprecedented accuracy. We demonstrate the destructive influences of stray magnetic fields caused by the current passing through feeding cables, and propose a correction method. Also, we show inter-individual differences in MRCDI measurements for two different current profiles, and compare the measurements with simulations based on individualized head models. The simulations of the current-induced magnetic fields show good agreement with in-vivo brain measurements.

Introduction

Accurate knowledge of the current flow in the human head induced by external sources is important to a wide range of neuroscience applications, for example targeting control in transcranial brain stimulation. MRCDI is a recently developed technique, which combines MRI with alternating currents to measure current flow in the human body. A first in-vivo MRCDI study of the human brain has been published recently (1), but the results appear to be severely influenced by stray magnetic field induced by the current passing through feeding cables. Here, we present uniquely reliable and unambiguous in-vivo measurements of weak electrical currents in the human brain.

Methods

Injected current that is synchronized with an MR sequence creates a magnetic field distribution inside the human body. The component of the current-induced magnetic field $\Delta B_{z,c}$ parallel to the scanner field causes small shifts in the precession frequency and modulates the phase of the MR signal. The accumulated phase is proportional to $\Delta B_{z,c}$, and can thus be used for $\Delta B_{z,c}$ and current flow calculations. We employed SSFP-FID (Fig.1a) with multi-gradient-echo readouts due to its high phase sensitivity, and used previously optimized sequence parameters (2) for human in-vivo MRCDI. 8 participants were recruited for two different MRCDI experiments (one subject participated twice). Before each experiment, T1-weighted (MPRAGE: number of slices Nsli=208, image matrix 256x256, voxel size (1 mm)^3, tip angle α=9˚, repetition time T_R=2700 ms, echo time T_E=3.63 ms, and inversion time T_I=1090 ms; PETRA: Nsli=320, image matrix 320x320, voxel size (0.9 mm)^3, α=6˚, T_R=3.61 ms, T_E=0.07 ms, T_I=0.5 s) and T2-weighted (SPACE: Nsli=208, image matrix 256x256, voxel size (1 mm)^3, T_R=3200 ms, and T_E=408 ms) structural scans were performed. The MPRAGE and SPACE scans were used to create individualized head models and for numerical simulations (3). The PETRA scan was used to image the feeding cables (covered with Play-Dough to improve the MR signal), as it enables imaging of materials with low T2. The currents were generated using an arbitrary waveform generator (33500B, KEYSIGHT Technologies, California, United States), amplified via an MR-conditional transcranial brain stimulator (DC-STIMULATOR PLUS, neuroConn GmbH, Germany), and injected via rubber electrodes attached to the scalp. First, we explored the influence of the cable-induced stray fields in four subjects. To emulate a realistic stray field, we placed a wire loop around the head, and measured $\Delta B_{z,c}$ with and without current. The stray field was calculated from the reconstructed cable paths by using the Biot-Savart Law, and the measurements were corrected correspondingly. Then, we explored the impact of employing two different current profiles, right-left (R-L) and anterior-posterior (A-P) in five subjects. The electrodes were attached close to the temporo-parietal junction for the R-L profile, and they connected the forehead and a position slightly above the inion for the A-P profile. The $\Delta B_{z,c}$ distributions were measured with I_c=1 mA. The measurements and simulations were used to reconstruct projected current density distributions (4,5). The experiments were performed with image matrix 112x90, voxel size 2x2x3 mm^3, α=30˚, number of multi-gradient-echo readout N_{GE}=7, bandwidth BW=75 Hz/pix, and T_R=120 ms, and repeated N_{meas}=24 times to increase the signal-to-noise-ratio.

Results and Discussion

The measured stray field due to cables is shown in Fig. 2b. The corrected $\Delta B_{z,c}$ images (Fig. 2c) and the $\Delta B_{z,c}$ images without current (Fig. 2d) are both near zero, which validates the correction method. Figure 3 shows the stray field influence for two different current profiles R-L and A-P, which dominates the results. The corrected results (Fig. 3c) clearly demonstrate the inter-individual $\Delta B_{z,c}$ differences. The first subject's $\Delta B_{z,c}$ measurements and simulations are exemplarily shown (Fig. 4a), and they agree well. The current estimated from measurements and from simulations are stronger in highly conductive regions, such as the longitudinal fissure and sulci (Fig. 4b). However, this is not seen when the uncorrected results are analyzed. Neglecting the stray fields hence compromises current flow estimation (~10% on average, and more locally).

Conclusion

The use of SSFP-FID with multi-gradient-echo readouts provides reliable MRCDI measurements, as systematic averaging of multi-echoes reduces detrimental effects (e.g. blood flow and motion). The cable-induced stray magnetic fields have a strong influence in $\Delta B_{z,c}$ measurements, which causes misestimating the current density distribution. Our correction method effectively eliminates the cable-induced stray magnetic fields. The corrected $\Delta B_{z,c}$ measurements and estimated current densities agree well with simulations, whereas uncorrected measurements do not. In short, this study is a uniquely reliable demonstration of human in-vivo brain MRCDI and can be used to improve the accuracy of the novel numerical simulations of transcranial brain stimulation.

Acknowledgements

The project is supported by Lundbeck foundation with grant number R118-A11308.

References

1. Kasinadhuni AK, Indahlastari A, Chauhan M, Schär M, Mareci TH, Sadleir RJ. Imaging of current flow in the human head during transcranial electrical therapy. Brain Stimul. 2017:1–9.

2. Göksu C, Scheffler K, Ehses P, Hanson LG, Thielscher A. Sensitivity Analysis of Magnetic Field Measurements for Magnetic Resonance Electrical Impedance Tomography (MREIT). Magn. Reson. Med. 2017. doi: 10.1002/mrm.26727.

3. Thielscher A, Antunes A, Saturnino GB. Field modeling for transcranial magnetic stimulation: A useful tool to understand the physiological effects of TMS? In: Proceedings of the Annual International Conference of the IEEE Engineering in Medicine and Biology Society, EMBS. ; 2015. pp. 222–225.

4. Park C, Lee B Il, Kwon OI. Analysis of recoverable current from one component of magnetic flux density in MREIT and MRCDI. Phys. Med. Biol. 2007;52:3001–13.

5. Ider YZ, Birgül Ö, Oran ÖF, Arıkan O, Hamamura MJ, Müftüler T. Fourier transform magnetic resonance current density imaging (FT-MRCDI) from one component of magnetic flux density. Phys. Med. Biol. 2010;55:3177–3199.

Figures

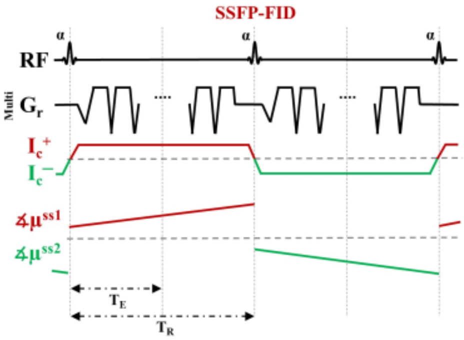

Figure 1. (a) Schematic diagram of the SSFP-FID sequence, which is composed of repetitive in-phase excitation pulses with constant tip angle and T_R. The current-induced phase of the transverse magnetization (∡μ) evolves in opposite directions in odd and even T_R periods, which results in two different steady-states with opposite phases. Multi-gradient-echo readouts (multi Gr, N_{GE} = 7) are used.

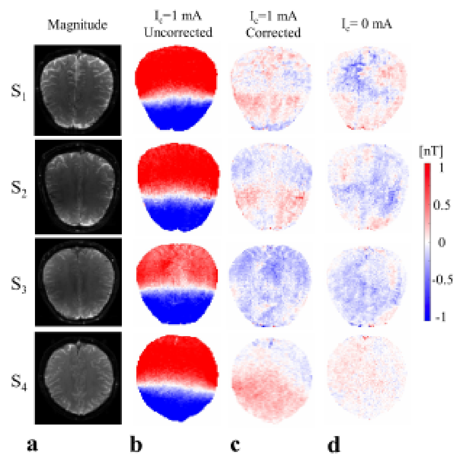

Figure 2. Correction of the cable-induced magnetic stray fields for SSFP-FID measurements (T_R=120 ms, N_{meas}=24) with multi-gradient-echo readouts in four subjects (no tissue currents). (a) Magnitude images. (b) Uncorrected $\Delta B_{z,c}$ images showing the stray field generated by the current flow in the wire loop around the head. (c) Corrected $\Delta B_{z,c}$ images, in which the stray field was calculated based on the reconstructed wire path and subtracted from the measured $\Delta B_{z,c}$. (d) $\Delta B_{z,c}$ images of the control measurements performed without current injection.

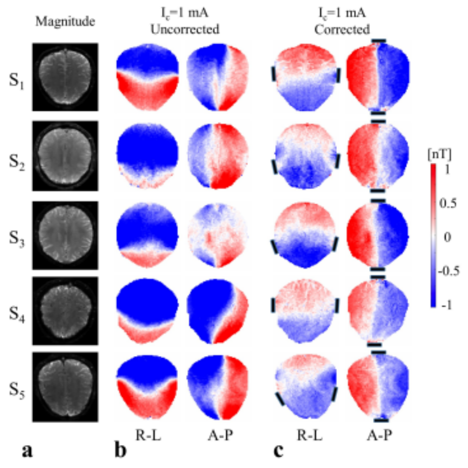

Figure 3. SSFP-FID measurements (T_R=120 ms, N_{meas}= 24) with multi-gradient-echo readouts of five subjects for the R-L and A-P electrode montages. (a) Magnitude images. (b) Uncorrected $\Delta B_{z,c}$ images (left column: R-L montage; right column: A-P montage). (c) Corrected $\Delta B_{z,c}$ images. The electrode positions are indicated as black boxes. Note that cable contributions dominate the uncorrected images.

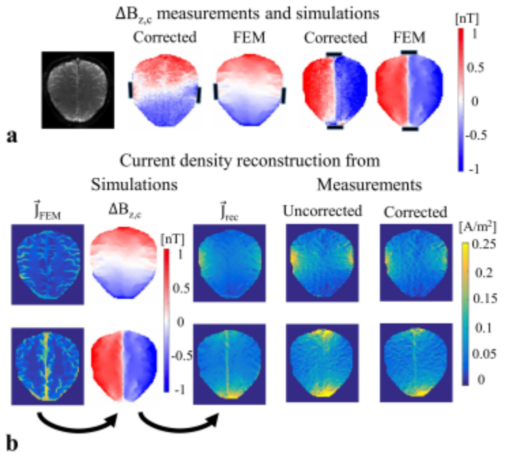

Figure 4. (a) SSFP-FID measurements and FEM simulations of the current-induced $\Delta B_{z,c}$ for the first subject. There are no artifacts observed in the MR magnitude images. Measurements and simulations agree well. (b) Please note that FEM simulations of current flow FEM are different than the estimated projected current density rec. The projected current was estimated from simulations that match corrected measurements well and demonstrate the strong current flow in sulci (R-L) and in the longitudinal fissure (A-P). rec estimated from uncorrected measurements deviate severely from the simulations, which is most visible near electrodes. Also, stronger currents in highly conductive regions disappear.

Proc. Intl. Soc. Mag. Reson. Med. 26 (2018)
0542